OCEAN CO_2 SEQUESTRATION EFFICIENCY FROM 3-D OCEAN MODEL COMPARISON

JAMES C. ORR and OLIVIER AUMONT
LSCE/CEA Saclay, CEA-CNRS and IPSL, Gif-sur-Yvette, France
ANDREW YOOL
Southampton Oceanography Centre (SOC), Southampton, UK
KASPER PLATTNER and FORTUNAT JOOS
Climate and Environmental Physics, Physics Institute, University of Bern (PIUB), Switzerland
ERNST MAIER-REIMER
Max Planck Institut fuer Meteorologie (MPIM), Hamburg, Germany
MARIE-FRANCE WEIRIG and REINER SCHLITZER
Alfred Wegener Institute for Polar and Marine Research (AWI), Bremerhaven, Germany
KEN CALDEIRA and MICHAEL WICKETT
Lawrence Livermore National Laboratory (LLNL), California, USA
RICHARD MATEAR
CSIRO, Hobart, Australia

ABSTRACT

The efficiency of sequestering CO_2 artificially in the deep ocean is not well known. To estimate uncertainties, we made standard simulations in a diverse group of seven ocean models. Each model discretizes the ocean into a 3-D array of grid cells, and each includes a standard description of the inorganic ocean carbon cycle. Injection simulations with seven injection sites per run were made separately for three different depths. At 3000 m, all models retained at least 97% of the total injected CO_2 at the end of the 100-year injection period; after 500 years, retention efficiency ranged from 48 to 82%. At 1500 m, retention efficiency was less (82-96% after 100 years; 28-57% after 500 years). At 800 m, it was less still (73-83% after 100 years; 15-38% after 500 years). For the 1500-m injection, San Francisco is generally the most efficient site, New York is the least efficient. For the 3000-m injection, differences between sites are smaller. Western boundary sites (New York and Tokyo) increased in efficiency more than other sites. In the 1500-m and 3000-m simulations, injected CO_2 is lost mostly from the Southern Ocean, except for CO_2 injected at 1500 m at New York, which is lost mostly from the North Atlantic.

INTRODUCTION

As one means to help mitigate rising levels of atmospheric CO_2, it has been proposed to sequester CO_2 generated by power plants in the deep ocean, instead of emitting it directly to the atmosphere, (Marchetti, 1977). The efficiency of such deep-ocean sequestration remains an open question. Ocean modelling studies provide the only means to estimate ocean sequestration efficiency. If CO_2 would be injected in the deep ocean, ocean circulation patterns would transport it typically quite far from the injection point before it would have a chance to reach the surface and be lost to the atmosphere through air-sea gas exchange. Such transport could require from centuries to a millennium, depending on the location of the injection point. Relatively simple 1-D vertical box models have been used to estimate the global efficiency of the ocean in retaining sequestered CO_2 (Hoffert et al., 1979). Such models instantly spread sequestered CO_2 globally throughout a given deep-ocean layer and thus are not suitable for estimating the efficiency at different injection sites. Conversely, site-specific injection simulations can be made with 3-D ocean models. Until now, only two 3-D models have been used to evaluate the efficiency of deep-ocean sequestration scenarios. These results were compared at two sites, and simulated efficiencies differed widely (Orr and Aumont, 1999). Here we describe the first results from a more extensive international effort to estimate both global and site-specific efficiencies. We have made standard simulations in a diverse

group of seven multi-dimensional ocean models. Model comparison allows us to provide a range of efficiency estimates. We have further relied on model-data $^{14}C/^{12}C$ comparison to help determine if real ocean behaviour would be bracketed by the range of simulated efficiencies.

MODELS AND SIMULATIONS

All seven models have global coverage with coarse-resolution grids, which do not resolve eddies. All models discretize the ocean in three dimensions, although the PIUB model is zonally averaged in each of the Atlantic, Pacific, and Indian basins. Four of the models (CSIRO, IPSL, LLNL, and SOC) describe the primitive equations (Bryan, 1969). The LSG model from MPIM is similar, but for computational efficiency, it neglects nonlinear terms in the advection equation. In the PIUB model, momentum equations are balanced between terms for the Coriolis force, horizontal pressure gradient, and zonal wind stress. The AWI model's circulation field is derived, with an adjoint method, from observed 3-D fields of hydrography, nutrients, and carbon. Models differ in their imposed wind stress and surface fluxes of heat and water. The AWI and PIUB models are forced with average annual conditions; the other five models are seasonal. Both LLNL and MPIM models are coupled with sub-models that describe the dynamics as well as the thermodynamics of sea ice.

Lateral subgrid-scale mixing is strictly horizontal in the MPI and PIUB models; conversely, lateral mixing is oriented along isopycnal surfaces in the CSIRO, IPSL, LLNL, and SOC models. All of those use some form of the eddy-induced velocity parameterisation of Gent et al. (1995), hereafter GM. To study sensitivity to lateral mixing we compared the standard IPSL model (with GM) to an identical version with only horizontal mixing (HOR). Vertical eddy diffusion is prescribed in the CSIRO, LLNL, MPIM, and PIUB models; the SOC model uses a Richardson number dependant scheme with a Kraus and Turner [1967] mixed layer; the IPSL model which uses a prognostic Turbulent Kinetic Energy scheme [Gaspar et al., 1990]. Advection schemes also differ. The CSIRO LLNL, and SOC models use the leapfrog CTCS scheme. The MPIM and PIUB models use upstream tracer advection, which contributes numerical diffusion both horizontally and vertically. The AWI model uses a weighted mean combination of CTCS and upstream schemes. The IPSL model uses the positive definite scheme known as MPDATA. Numerous other differences also exist. More complete model descriptions can be found elsewhere: AWI (Schlitzer, 1999), CSIRO (Matear and Hirst, 1999), IPSL (Madec and Imbard, 1996), LLNL (Caldeira, 2000), MPIM (Maier-Reimer, 1993), PIUB (Stocker et al., 1992), and SOC (Gordon et al., 2000).

Simulation protocols were designed as part of the international project known as GOSAC (Global Ocean Storage of Anthropogenic Carbon) in conjunction with OCMIP (Ocean Carbon-Cycle Model Intercomparison Project). To conserve computing resources, our injection protocol makes two simplifications. First, all models simulations were made without accounting for the influence of marine biota. Such a simplification affects results by less than 5% (Bacastow and Dewey, 1996; Orr and Aumont, 1999). Second, only DIC was transported. Thus we neglected calcite dissolution, which is considered negligible for several centuries after injection (Archer et al., 1998). For air-sea gas exchange, we used the standard boundary conditions specified for the second phase of OCMIP: (1) the gas transfer coefficient from Wanninkhof (1992); (2) wind speeds from remotely sensed SSMI data (Boutin and Etcheto, 1997); and (3) fractional sea ice cover (Walsh, 1978; Zwally et al., 1983). Carbonate chemistry equilibria constants and CO_2 solubility are from DOE (1994).

Models were integrated to obtain preindustrial conditions (atmospheric pCO_2=278 ppm), then forced to follow observed atmospheric CO_2 during 1765-2000. Subsequently during 2000-2500, models were forced to follow IPCC future scenario S650, which eventually stabilises atmospheric pCO_2 at 650 ppm (Fig. 1a). Injection occurred only during 2000-2100, with 0.1 Pg C year^{-1} being

injected just offshore at each of seven sites (Bay of Biscay, Bombay, Jakarta, New York, Rio de Janeiro, San Francisco, and Tokyo).

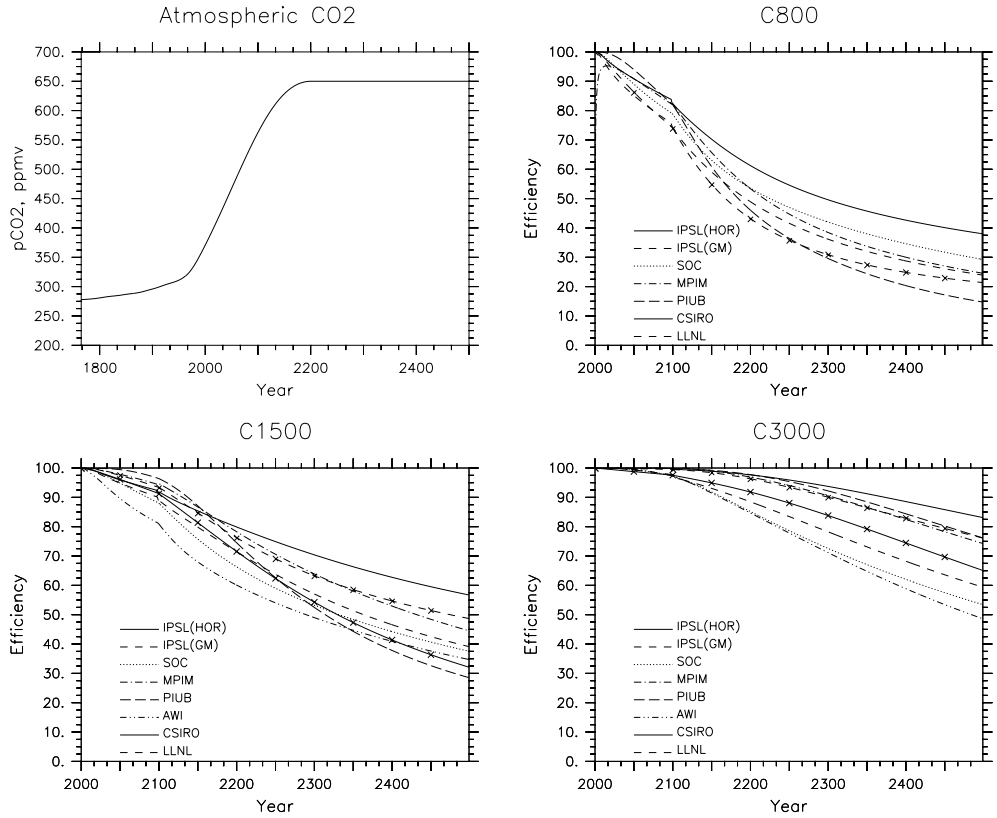

Figure 1: (a) IPCC Atmospheric CO_2 concentration scenario prescribed in all models simulations reported here. Conversely, previous work prescribed fossil emissions. Had we done that here, anthropogenic air-sea fluxes would have also differed between models, thereby complicating interpretation of results. Our resulting Injection Efficiency Ei (the mass of injected CO_2 that remains in the ocean / the total injected since the start of injection) for injection at 800 m, (b) 1500 m, and (c) 3000 m. Conversely Orr and Aumont (1999) calculated (1) the Total Efficiency Et (reduction in atmospheric CO_2 /reduction in emissions) and (2) the Permanent Efficiency Ep (Total Efficiency / Total Efficiency for permanent sequestration). Our global Ei is similar to Orr and Aumont's Ep and substantially larger than their Et.

For each injection simulation, we used ten separate DIC tracers: seven were used to track, individually, the seven DIC plumes extending from the seven injection sites; the three others were used to account for a control run, invasion of anthropogenic CO_2, and a permanent sequestration scenario. Orr and Aumont (1999) found that nonlinearities due to this multi-tracer approach were negligible, relative to a single-tracer approach. Detailed protocols, boundary conditions, and example code for making these simulations can be found in the Injection-HOWTO document that is available on the OCMIP web page (http://www.ipsl.jussieu.fr/OCMIP).

RESULTS

In the immediate vicinity of the injection sites, the concentration of dissolved inorganic carbon (DIC) increases substantially. In year 2099, the last year of the 100-year injection period, perturbations range from about 10% of to twice the natural background concentrations (around 2000 μmol L^{-1}), depending on the model and the injection site. Local differences in perturbed DIC concentrations are controlled by model resolution and ocean transport. The AWI and MPIM models produce the highest injection site DIC concentrations. As a sensitivity test, we multiplied the MPIM model's explicit horizontal eddy diffusion coefficient (200 m^2 s^{-1}) by three. Resulting injection site DIC concentrations were reduced by more than half; yet, there were only negligible changes in the efficiency of the ocean retention of injected CO_2.

Simulations confirmed expectations that deeper injection is more efficient (Fig. 1). Injection at 3000 m is at least 85% efficient in all models in year 2200 (i.e., 100 years after the end of the 100-year injection period); at the same time, 1500-m injection is 60-80% efficient and 800-m injection is 42-61% efficient. A sensitivity test in the SOC model reveals that continuing injection after 2100 increases global efficiency from 66% to 77% in 2200 and from 38% to 58% in 2500.

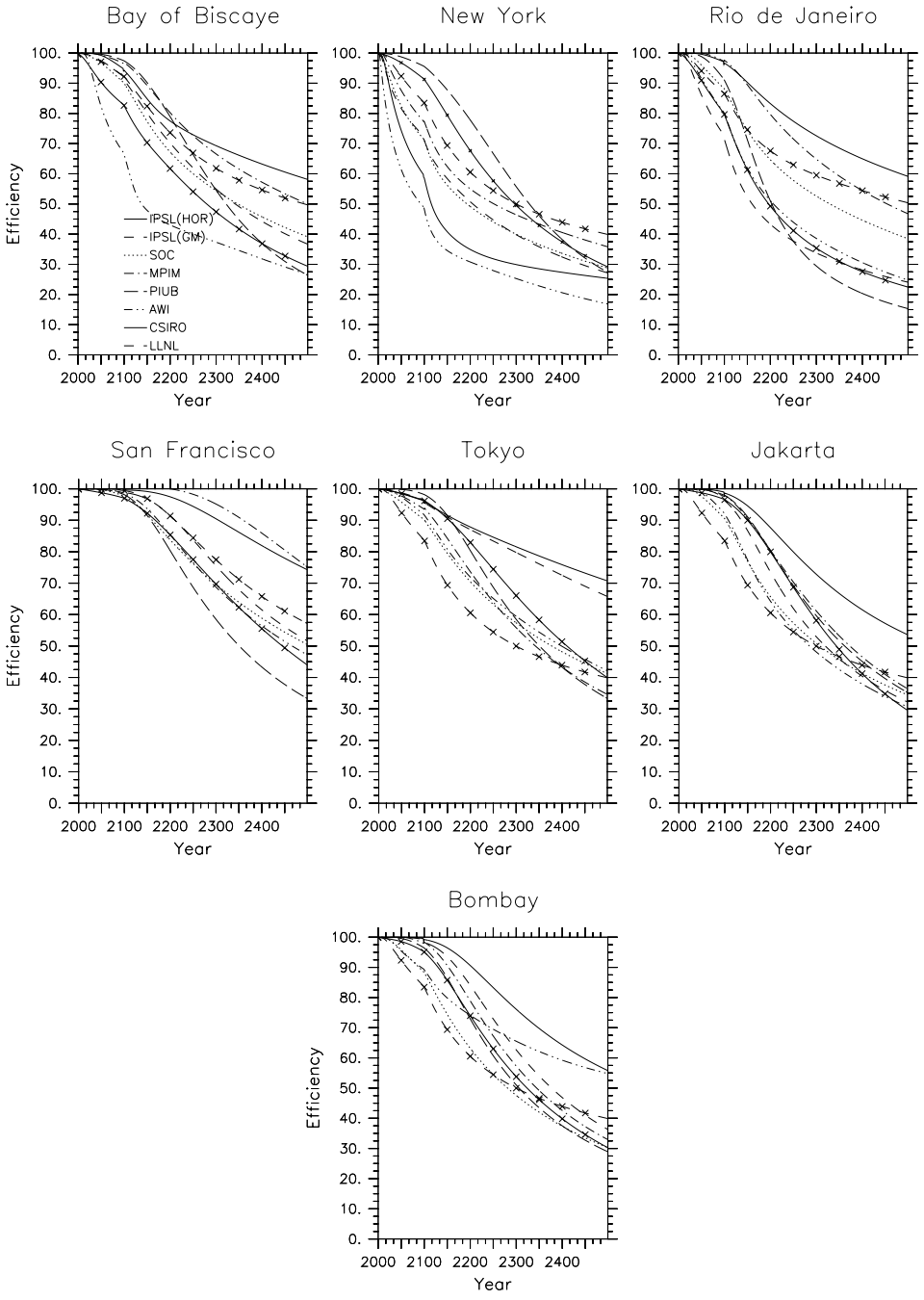

Figure 2: Injection efficiencies (Ei) for the 1500-m injection at each of the seven injection sites.

Comparison of the efficiency between sites for the 1500-m injection reveals large differences (Fig. 2). Most of the models simulate that injection in the Pacific (San Francisco, Tokyo) is more efficient than in the Atlantic (New York, Bay of Biscay, and Rio de Janeiro). Most models also simulate that injection in the Indian Ocean yields intermediate efficiencies. All but the zonal-average model (PIUB) simulate that injection at San Francisco is most efficient. Five of the eight model runs simulate that injection at New York is least efficient. Much of that injected CO_2 is transported northward and lost mainly from the North Atlantic (Fig. 3).

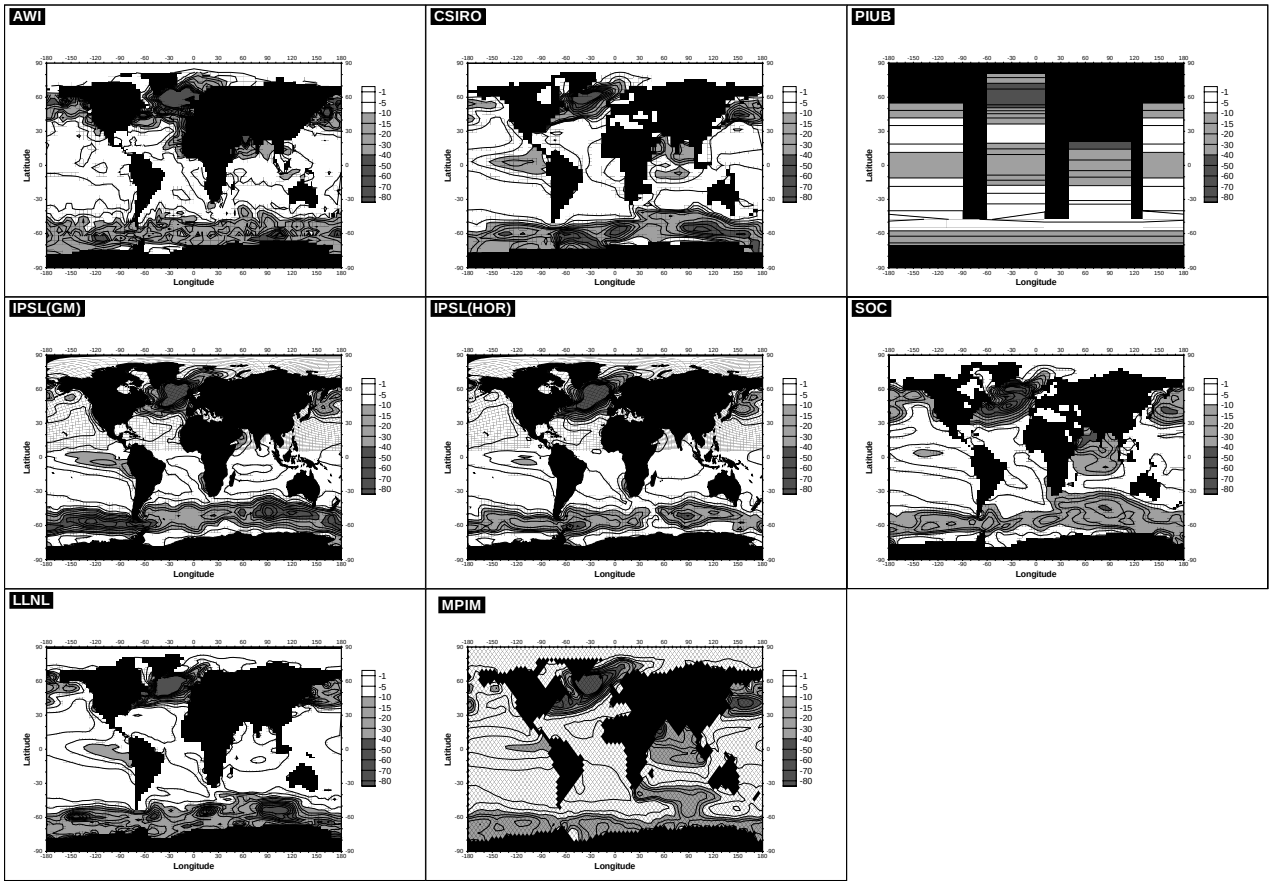

Figure 3: The cumulative loss of injected CO_2 (mol m^{-2}) from the beginning of the 100-year injection period (year 2000) until the end of the simulation (year 2500). When integrated spatially, most of the loss occurs south of 30S, which covers 31% of the surface area of the global ocean. Negative values represent fluxes from ocean to atmosphere.

For the 3000-m injection, all sites became more efficient, and injection site efficiencies are more tightly grouped for each model. Western boundary sites (New York and Tokyo) improved more in efficiency relative to other sites. For injection at 3000 m off New York, less CO_2 is able to escape from the North Atlantic. Instead more of it moves southward, along a longer pathway, for eventual loss from the Southern Ocean. All other sites in the 1500-m and 3000-m injection simulations lose most of their CO_2 from the Southern Ocean (Fig. 3).

DISCUSSION

One must validate injection simulations indirectly. Radiocarbon (^{14}C) has been measured throughout the ocean as the $^{14}C/^{12}C$ ratio. Its radioactive decay provides an estimate of the age of deep waters, which should be related to injection efficiency. OCMIP has compared simulations of natural $^{14}C/^{12}C$ in our models with the global $^{14}C/^{12}C$ dataset from WOCE and GEOSECS. Pacific and Indian Ocean deep waters are too old in the IPSL(HOR) model and too young in the AWI model. Thus the AWI model appears to provide a lower limit and the IPSL(HOR) model an upper limit and for deep sequestration efficiency in these basins. These same two models bracket all other model results for the global efficiency of the 3000-m injection. More validation with $^{14}C/^{12}C$ is necessary to evaluate general model behaviour in the Atlantic Ocean. In similar fashion, WOCE has also produced a global database of the Helium-3/Helium-4 ratio. Unlike the more homogenous sea-surface input of $^{14}C/^{12}C$, $^{3}He/^{4}He$ is injected at point sources in the deep ocean along mid-ocean ridges and is eventually lost to the atmosphere through air-sea gas exchange. As such, $^{3}He/^{4}He$ is similar to CO_2 injected in the deep ocean. Future model-data comparison with $^{3}He/^{4}He$ should be a high priority for those making ocean model simulations of CO_2 injection. Improved ability to

validate models would come from efforts to measure $^{14}C/^{12}C$ and $^{3}He/^{4}He$ near potential injection sites as well as where injected CO_2 is lost from the ocean (e.g., the Southern Ocean).

ACKNOWLEDGEMENTS

Discussions initiated by B. Ormerod, P. Freund, and J. Sarmiento incited this study. We thank B. Ormerod, H. Drange, J. Davison, B. Bacastow, C. S. Wong, P. Haugan, and G. Nihous for suggestions regarding ocean injection sites, depths, and rates. We are grateful to J. Davison for discussions throughout this work. Analysis presented here was funded by the IEA Greenhouse Gas R&D Programme. The AWI, IPSL, MPIM, and SOC modelling groups were funded by the EC Environment and Climate Programme (Contract ENV4-CT97-0495). PIUB was funded by the Swiss NSF and the Swiss Fed. Office for Science and Education (grant 97.0414). LLNL was funded through the U.S. DOE Ocean Carbon Sequestration Center. Opinions which may be drawn from this work do not necessarily reflect those of any of the funding agencies.

REFERENCES

Archer D, Kheshgi HS, and Maier-Reimer E (1998). Dynamics of fossil fuel CO_2 neutralisation by marine $CaCO_3$, Global Biogeochem. Cycles, 12, 259--276.

Bacastow, RB and Dewey RK (1996). Effectiveness of CO_2 sequestration in the post-industrial ocean, Energy Convers. Mgmt., 37, 1079--1086.

Boutin J and Etcheto J (1997). Long-term variability of the air-sea CO_2 exchange coefficient: Consequences for the CO_2 fluxes in the equatorial Pacific Ocean, Global Biogeochem. Cycles, 11(3), 453--470.

Bryan K, A numerical method for the study of the circulation of the world ocean, J. Comput. Phys., 4(3), 347--376, 1969.

Caldeira K and Duffy PB (2000). The role of the southern ocean in uptake and storage of anthropogenic carbon dioxide, Science, 287, 620--622.

DOE (1994). Handbook of methods for the analysis of the various parameters of the carbon dioxide system in seawater; version 2, Dickson, AG and Goyet C, eds., ORNL/CDIAC-74.

Gaspar P, Gregorius Y, and Lefevre J-M (1990). A simple eddy kinetic energy model for simulations of oceanic vertical mixing tests at Station Papa and Long-Term Upper Ocean Study Site, J. Geophys. Res., 95, 16179--16193.

Gent PR, Willebrand J, McDougall TJ, and McWilliams JC (1995). Parameterizing eddy-induced tracer transports in ocean circulation models, J. Phys. Oceanogr., 25, 463—474.

Gordon C, Senior CA, Banks H. Gregory JM, Johns TC, Mitchell JFB, and Wood RA (2000). The simulation of SST, sea ice extents and ocean heat transport in a version of the Hadley centre coupled model without flux adjustments, Clim. Dyn,., 16, 147-168.

Hoffert MI, Wey Y-C, Callegari AJ, and Broecker WS (1979). Atmospheric response to deep-sea injections of fossil-fuel carbon dioxide, Climatic Change, 2, 53--68.

Kraus E and Turner J (1967). A one dimensional model of the seasonal thermocline, part II, Tellus, 19, 98--105.

Madec G and Imbard M (1996). A global ocean mesh to overcome the North Pole singularity, Clim. Dyn., 12, 381--388.

Maier-Reimer E (1993). Geochemical cycles in an ocean general circulation model: Preindustrial tracer distributions, Global Biogeochem. Cycles, 7(3), 645--677.

Marchetti C (1977). On geoengineering and the CO_2 problem, Clim. Change, 1, 59--68.

Matear RJ and Hirst AC (1999). Climate change feedback on the future oceanic CO_2 uptake, Tellus, 51B, 722--733.

Orr JC and Aumont O (1999). Exploring the capacity of the ocean to retain artificially sequestered CO_2, in Greenhouse Gas Control Technologies, edited by Eliasson BE, Reimer P, and Wokaun A, pp. 281--286, Elsevier Science Ltd..

Schlitzer R (1999). Inverse methods in global biogeochemical cycles, in Applying the adjoint method for global biogeochemical modelling, edited by Kasibhatla P, Heimann M, Hartley D, Mahowald N, Prinn R, and Rayner P, volume 114 of Geophys. Monograph Series, pp. 107--124, Washington D.C., AGU.

Walsh J (1978). A data set on northern hemisphere sea ice extent, 1953-1976, Glaciological data, World Data Cent. A for Glaciol. [Snow and Ice], Boulder, Colorado, Report GD-2.

Wanninkhof R (1992). Relationship between wind speed and gas exchange over the ocean, J. Geophys. Res., 97, 7373--7382.

Stocker TF , Wright DG, Mysak LA (1992). A zonally averaged, coupled ocean-atmosphere model for paleoclimate studies, J. Climate, 5, 773—797, 1992.

Zwally HJ, Comiso J, Parkinson C, Campbell W., Carsey F, and Gloerson P (1983). Antarctic sea ice, 1973-1976: Satellite passive microwave observations, NASA.